AIMS Mathematics, 8(8): 19794–19815.
DOI: 10.3934/math.20231009
Received: 31 January 2023
Revised: 24 May 2023
Accepted: 06 June 2023
Published: 13 June 2023

http://www.aimspress.com/journal/Math

Research article

Split-step quintic B-spline collocation methods for nonlinear Schrödinger equations

Shanshan Wang[1,2,*]

[1] College of Mathematics, Nanjing University of Aeronautics and Astronautics, Nanjing 211106, China

[2] Key Laboratory of Mathematical Modelling and High Performance Computing of Air Vehicles (NUAA), MIIT, Nanjing 211106, China

* **Correspondence:** Email: wangss@nuaa.edu.cn.

Abstract: Split-step quintic B-spline collocation (SS5BC) methods are constructed for nonlinear Schrödinger equations in one, two and three dimensions in this paper. For high dimensions, new notations are introduced, which make the schemes more concise and achievable. The solvability, conservation and linear stability are discussed for the proposed methods. Numerical tests are carried out, and the present schemes are numerically verified to be convergent with second-order in time and fourth-order in space. The conserved quantity is also computed which agrees with the exact one. And solitary waves in one, two and three dimensions are simulated numerically which coincide with the exact ones. The SS5BC scheme is compared with the split-step cubic B-spline collocation (SS3BC) method in the numerical tests, and the former scheme is more efficient than the later one. Finally, the SS5BC scheme is also applied to compute Bose-Einstein condensates.

Keywords: split-step; quintic B-spline collocation; nonlinear Schrödinger equation; numerical experiment; convergence order; conservation law; soliton; Bose-Einstein condensate
Mathematics Subject Classification: 65M70, 35Q55, 35Q51

1. Introduction

Efficient and reliable numerical methods are always urgently needed for nonlinear multi-dimensional problems due to the mass storage and the high computation cost. The split-step method, also known as the time-splitting method, is one kind of efficient skills for solving nonlinear parabolic or Schrödinger-type problems in multi-dimensions.

The split-step skill could be efficiently combined with the (compact) finite difference method [1, 2], the finite element method [3, 4], the spectral/pseudospectral method [5, 6], et al. So the authors

of [7] try to combine the skill with the cubic B-spline collocation (3BC) approach, and they formulate the split-step 3BC (SS3BC) method sucessfully. However, the SS3BC method is just second-order accuracy in space, and there is no numerical analysis in [7]. Genarally speaking, the 3BC method has second-order accuracy, and the quintic B-spline collocation (5BC) method is fourth-order [8]. Thus, split-step 5BC (SS5BC) methods are constructed in this paper to improve the accuracy in space, and some analyses are also given.

In this paper, we consider the nonlinear Schrödinger (NLS) equations as follows

$$i\frac{\partial u}{\partial t}(\mathbf{x},t) + \alpha\Delta u(\mathbf{x},t) + V(\mathbf{x},t)u(\mathbf{x},t) + \beta|u(\mathbf{x},t)|^2u(\mathbf{x},t) = 0,\ \mathbf{x}\in\mathbf{R}^d, t\in(0,T], \tag{1.1}$$

with the initial condition

$$u(\mathbf{x},0) = u_0(\mathbf{x}),\ \mathbf{x}\in\mathbf{R}^d, \tag{1.2}$$

and the periodic boundary condition

$$u(\mathbf{x}+\mathbf{L},t) = u(\mathbf{x},t),\ \mathbf{x}\in\mathbf{R}^d, t\in[0,T], \tag{1.3}$$

where $\mathbf{L} = (L_x, L_y, L_z)$, and L_x, L_y and L_z are the periodic lengths respectively in the x, y and z direction. $u(\mathbf{x},t)$ is an unknown complex function, $V(\mathbf{x},t)$ and $u_0(\mathbf{x})$ are given functions, α,β are real constants, $T > 0$ and $i^2 = -1$.

Computing the inner product of Eq (1.1) with u, and taking the imaginary part, one obtains the following conservation law

$$Q(t) = \int_{\mathbf{R}^d}|u(\mathbf{x},t)|^2d\mathbf{x} = \int_{\mathbf{R}^d}|u(\mathbf{x},0)|^2d\mathbf{x} = Q(0). \tag{1.4}$$

The rest of this paper is organized as follows. In Section 2, some preliminaries are introduced, and SS5BC methods are constructed in Section 3. In Section 4, solvability, conservation and linear stability of the schemes are discussed. Numerical experiments are carried out in Section 5, and the present methods are applied to study BECs in Section 6. Finally, some conclusions are given in Section 7.

2. Preliminaries

We consider Eq (1.1) within $\mathbf{x}\in\Omega_d\subseteq\mathbf{R}^d$. Take $\Omega_3 = [x_L, x_R]\times[y_L, y_R]\times[z_L, z_R]$, and $x_R - x_L = L_x, y_R - y_L = L_y, z_R - z_L = L_z$. Let $\{x_k\}_{k=0}^{N_x}\otimes\{y_l\}_{l=0}^{N_y}\otimes\{z_m\}_{m=0}^{N_z}$ be the partition of Ω_3, such that

$$x_j = x_L + jh_x, y_k = y_L + kh_y, z_l = z_L + lh_z, j = 1,2,\cdots,N_x, k = 1,2,\cdots,N_y, l = 1,2,\cdots,N_z,$$

where $h_x = (x_R - x_L)/N_x, h_y = (y_R - y_L)/N_y$ and $h_z = (z_R - z_L)/N_z$ are the step sizes in space, and N_x, N_y and N_z are positive integers. Obviously, Ω_1 and Ω_2 are reduced forms of Ω_3 which could also be partitioned. We divide the interval $[0,T]$ by the partition $\{t_n\}_{n=0}^{N_t}$, where $t_n = n\tau$, $\tau = T/N_t$ is the step size in time, and N_t is a positive integer.

For one dimension, let $\{B_j(x)\}_{j=-2}^{N_x+2}$ be the quintic B-spline basis functions [8] on the knots $\{x_j\}_{j=0}^{N_x}$,

such that

$$B_j(x) = \frac{1}{h^5}\begin{cases} (x-x_{j-3})^5, & x \in [x_{j-3}, x_{j-2}], \\ (x-x_{j-3})^5 - 6(x-x_{j-2})^5, & x \in [x_{j-2}, x_{j-1}], \\ (x-x_{j-3})^5 - 6(x-x_{j-2})^5 + 15(x-x_{j-1})^5, & x \in [x_{j-1}, x_j], \\ (x-x_{j-3})^5 - 6(x-x_{j-2})^5 + 15(x-x_{j-1})^5 - 20(x-x_j)^5, & x \in [x_j, x_{j+1}], \\ (x-x_{j-3})^5 - 6(x-x_{j-2})^5 + 15(x-x_{j-1})^5 - 20(x-x_j)^5 & \\ +15(x-x_{j+1})^5, & x \in [x_{j+1}, x_{j+2}], \\ (x-x_{j-3})^5 - 6(x-x_{j-2})^5 + 15(x-x_{j-1})^5 - 20(x-x_j)^5 & \\ +15(x-x_{j+1})^5 - 6(x-x_{j+2})^5, & x \in [x_{j+2}, x_{j+3}], \\ 0, & \text{otherwise.} \end{cases} \tag{2.1}$$

Similarly, we can define $\{B_k(y)\}_{k=-2}^{N_y+2}$ and $\{B_l(z)\}_{l=-2}^{N_z+2}$ as the basis functions on the knots $\{y_k\}_{k=0}^{N_y}$ and $\{z_l\}_{l=0}^{N_z}$, respectively.

A global approximation solution $U_N(x,t)$ of the exact solution $u(x,t)$ could be expressed in terms of the quintic B-spline as

$$U_N(x,t) = \sum_{j=-2}^{N_x+2} \delta_j(t) B_j(x), \tag{2.2}$$

where $\delta_j(t)$ are unknown time dependent parameters which should be determined. According to the property of the quintic B-spline (2.1), we can get the nodal values as follows:

$$U_N(x_j,t) = \delta_{j-2}(t) + 26\delta_{j-1}(t) + 66\delta_j(t) + 26\delta_{j+1}(t) + \delta_{j+2}(t), \tag{2.3}$$

$$\frac{\partial U_N}{\partial x}(x_j,t) = \frac{5}{h_x}\left[-\delta_{j-2}(t) - 10\delta_{j-1}(t) + 10\delta_{j+1}(t) + \delta_{j+2}(t)\right], \tag{2.4}$$

$$\frac{\partial^2 U_N}{\partial x^2}(x_j,t) = \frac{20}{h_x^2}\left[\delta_{j-2}(t) + 2\delta_{j-1}(t) - 6\delta_j(t) + 2\delta_{j+1}(t) + \delta_{j+2}(t)\right], \tag{2.5}$$

$$\frac{\partial^3 U_N}{\partial x^3}(x_j,t) = \frac{60}{h_x^3}\left[-\delta_{j-2}(t) + 2\delta_{j-1}(t) - 2\delta_{j+1}(t) + \delta_{j+2}(t)\right], \tag{2.6}$$

$$\frac{\partial^4 U_N}{\partial x^4}(x_j,t) = \frac{120}{h_x^4}\left[\delta_{j-2}(t) - 4\delta_{j-1}(t) + 6\delta_j(t) - 4\delta_{j+1}(t) + \delta_{j+2}(t)\right], \tag{2.7}$$

where $j = 0, 1, 2, \cdots, N_x$.

For two dimensions, an approximation solution $U_N(x,y,t)$ could be expressed as

$$U_N(x,y,t) = \sum_{j=-2}^{N_x+2}\sum_{k=-2}^{N_y+2} \delta_{jk}(t) B_j(x) B_k(y), \tag{2.8}$$

where $\delta_{jk}(t)$ are unknown time dependent parameters. According to (2.1), we can get the nodal value $U_N(x_j,y_k,t)$ as

$$\begin{aligned} U_N(x_j,y_k,t) \;=\; & [\delta_{j-2,k-2}(t) + 26\delta_{j-2,k-1}(t) + 66\delta_{j-2,k}(t) + 26\delta_{j-2,k+1}(t) + \delta_{j-2,k+2}(t)] \\ & +26[\delta_{j-1,k-2}(t) + 26\delta_{j-1,k-1}(t) + 66\delta_{j-1,k}(t) + 26\delta_{j-1,k+1}(t) + \delta_{j-1,k+2}(t)] \\ & +66[\delta_{j,k-2}(t) + 26\delta_{j,k-1}(t) + 66\delta_{j,k}(t) + 26\delta_{j,k+1}(t) + \delta_{j,k+2}(t)] \end{aligned}$$

$$+26[\delta_{j+1,k-2}(t) + 26\delta_{j+1,k-1}(t) + 66\delta_{j+1,k}(t) + 26\delta_{j+1,k+1}(t) + \delta_{j+1,k+2}(t)]$$
$$+[\delta_{j+2,k-2}(t) + 26\delta_{j+2,k-1}(t) + 66\delta_{j+2,k}(t) + 26\delta_{j+2,k+1}(t) + \delta_{j+2,k+2}(t)], \quad (2.9)$$

where $j = 0, 1, 2, \cdots, N_x$ and $k = 0, 1, 2, \cdots, N_y$. Unfortunately, Eq (2.9) is complicated, and it is two-dimensional which goes against the dimensionality reduction by the splitting method.

For simplicity, new notations $\tilde{\delta}_{j,k}(t)$ and $\hat{\delta}_{j,k}(t)$ are introduced as follows

$$\tilde{\delta}_{j,k}(t) = \delta_{j,k-2}(t) + 26\delta_{j,k-1}(t) + 66\delta_{j,k}(t) + 26\delta_{j,k+1}(t) + \delta_{j,k+2}(t), \quad (2.10)$$
$$\hat{\delta}_{j,k}(t) = \delta_{j-2,k}(t) + 26\delta_{j-1,k}(t) + 66\delta_{j,k}(t) + 26\delta_{j+1,k}(t) + \delta_{j+2,k}(t). \quad (2.11)$$

So Eq (2.9) could be rewritten as

$$U_N(x_j, y_k, t) = \tilde{\delta}_{j-2,k}(t) + 26\tilde{\delta}_{j-1,k}(t) + 66\tilde{\delta}_{j,k}(t) + 26\tilde{\delta}_{j+1,k}(t) + \tilde{\delta}_{j+2,k}(t), \quad (2.12)$$

or

$$U_N(x_j, y_k, t) = \hat{\delta}_{j,k-2}(t) + 26\hat{\delta}_{j,k-1}(t) + 66\hat{\delta}_{j,k}(t) + 26\hat{\delta}_{j,k+1}(t) + \hat{\delta}_{j,k+2}(t). \quad (2.13)$$

Obviously, either Eq (2.12) or Eq (2.13) is more concise than Eq (2.9). The advantage of the new writing will also be shown in the following sections.

For three dimensions, an approximation solution $U_N(x, y, z, t)$ could be expressed as

$$U_N(x, y, z, t) = \sum_{j=-2}^{N_x+2} \sum_{k=-2}^{N_y+2} \sum_{l=-2}^{N_z+2} \delta_{jkl}(t) B_j(x) B_k(y) B_l(z), \quad (2.14)$$

where $\delta_{jkl}(t)$ are unknown time dependent parameters.

Denote

$$\begin{aligned}
\tilde{\delta}_{j,k,l}(t) = & \left(\delta_{j,k-2,l-2}(t) + 26\delta_{j,k-2,l-1}(t) + 66\delta_{j,k-2,l}(t) + 26\delta_{j,k-2,l+1}(t) + \delta_{j,k-2,l+2}(t)\right) \\
& +26\left(\delta_{j,k-1,l-2}(t) + 26\delta_{j,k-1,l-1}(t) + 66\delta_{j,k-1,l}(t) + 26\delta_{j,k-1,l+1}(t) + \delta_{j,k-1,l+2}(t)\right) \\
& +66\left(\delta_{j,k,l-2}(t) + 26\delta_{j,k,l-1}(t) + 66\delta_{j,k,l}(t) + 26\delta_{j,k,l+1}(t) + \delta_{j,k,l+2}(t)\right) \\
& +26\left(\delta_{j,k+1,l-2}(t) + 26\delta_{j,k+1,l-1}(t) + 66\delta_{j,k+1,l}(t) + 26\delta_{j,k+1,l+1}(t) + \delta_{j,k+1,l+2}(t)\right) \\
& +\left(\delta_{j,k+2,l-2}(t) + 26\delta_{j,k+2,l-1}(t) + 66\delta_{j,k+2,l}(t) + 26\delta_{j,k+2,l+1}(t) + \delta_{j,k+2,l+2}(t)\right),
\end{aligned}$$

where the first subscript j related to x direction is fixed. Similarly, $\hat{\delta}_{j,k,l}(t)$ related to y direction and $\check{\delta}_{j,k,l}(t)$ related to z direction could be defined, where the second subscript k and the third subscript l are respectively fixed. Therefore, the nodal value $U_N(x_j, y_k, z_l, t)$ could be written as

$$\begin{aligned}
U_N(x_j, y_k, z_l, t) &= \tilde{\delta}_{j-2,k,l}(t) + 26\tilde{\delta}_{j-1,k,l}(t) + 66\tilde{\delta}_{j,k,l}(t) + 26\tilde{\delta}_{j+1,k,l}(t) + \tilde{\delta}_{j+2,k,l}(t) \\
&= \hat{\delta}_{j,k-2,l}(t) + 26\hat{\delta}_{j,k-1,l}(t) + 66\hat{\delta}_{j,k,l}(t) + 26\hat{\delta}_{j,k+1,l}(t) + \hat{\delta}_{j,k+2,l}(t) \\
&= \check{\delta}_{j,k,l-2}(t) + 26\check{\delta}_{j,k,l-1}(t) + 66\check{\delta}_{j,k,l}(t) + 26\check{\delta}_{j,k,l+1}(t) + \check{\delta}_{j,k,l+2}(t). \quad (2.15)
\end{aligned}$$

3. Numerical methods

Firstly, the second-order Strang splitting [9, 10] is applied, and Eq (1.1) could be separated as

$$i\frac{\partial u}{\partial t}(\mathbf{x},t)+\frac{1}{2}V(\mathbf{x},t)u(\mathbf{x},t)+\frac{\beta}{2}|u(\mathbf{x},t)|^2u(\mathbf{x},t)=0, \tag{3.1}$$

$$i\frac{\partial u}{\partial t}(\mathbf{x},t)+\alpha\Delta u(\mathbf{x},t)=0, \tag{3.2}$$

$$i\frac{\partial u}{\partial t}(\mathbf{x},t)+\frac{1}{2}V(\mathbf{x},t)u(\mathbf{x},t)+\frac{\beta}{2}|u(\mathbf{x},t)|^2u(\mathbf{x},t)=0. \tag{3.3}$$

So Eq (1.1) could be approximately solved within $t\in[t_n,t_{n+1}]$ by solving Eqs (3.1)–(3.3) in sequence.

Multipling Eq (3.1) by $\bar{u}$ and taking the imaginary part, it follows that

$$\frac{1}{2}\frac{\partial}{\partial t}|u|^2=0.$$

Thus $|u|^2$ in Eq (3.1) is independent of t. So one can take $|u(\mathbf{x},t)|^2=|u(\mathbf{x},t_n)|^2$. Consequently, it follows from Eq (3.1) that

$$u(\mathbf{x},t)=u(\mathbf{x},t_n)\exp\left\{\frac{i}{2}\left[\int_{t_n}^{t}V(\mathbf{x},t)dt+\beta(t-t_n)|u(\mathbf{x},t_n)|^2\right]\right\}, \tag{3.4}$$

where $t\in[t_n,t_{n+1}]$. Equation (3.3) could be solved similarly.

3.1. One-dimensional (1D) scheme

For $d=1$, Eq (3.2) could be written as

$$i\frac{\partial u}{\partial t}(x,t)+\alpha\frac{\partial^2 u}{\partial x^2}(x,t)=0. \tag{3.5}$$

Applying the Crank-Nicolson scheme within $t\in[t_n,t_{n+1}]$, one obtains

$$i\frac{U_N^{n+1}(x)-U_N^n(x)}{\tau}+\frac{\alpha}{2}\left[U_{Nxx}^{n+1}(x)+U_{Nxx}^n(x)\right]=0,$$

where $U_N^n(x)$ is the approximation of $u(x,t_n)$. Taking $x=x_j$, it follows from Eqs (2.3) and (2.5) that

$$(i+10\alpha r_x)(\delta_{j-2}^{n+1}+\delta_{j+2}^{n+1})+(26i+20\alpha r_x)(\delta_{j-1}^{n+1}+\delta_{j+1}^{n+1})+(66i-60\alpha r_x)\delta_j^{n+1}=iU_N^n(x_j)-\frac{\tau\alpha}{2}U_{Nxx}^n(x_j),$$

where $r_x=\tau/h_x^2$.

Consequently, Eqs (3.1)–(3.3) for $d=1$ could be solved in sequence as follows

$$U_N^{n+1,1}(x)=U_N^n(x)\exp\left\{\frac{i}{2}\left[\int_{t_n}^{t_{n+1}}V(x,t)dt+\tau\beta|U_N^n(x)|^2\right]\right\}, \tag{3.6}$$

$$\begin{aligned}&(i+10\alpha r_x)(\delta_{j-2}^{n+1,2}+\delta_{j+2}^{n+1,2})+(26i+20\alpha r_x)(\delta_{j-1}^{n+1,2}+\delta_{j+1}^{n+1,2})+(66i-60\alpha r_x)\delta_j^{n+1,2}\\&=iU_N^{n+1,1}(x_j)-\frac{\tau\alpha}{2}U_{Nxx}^{n+1,1}(x_j),\end{aligned} \tag{3.7}$$

$$U_N^{n+1}(x)=U_N^{n+1,2}(x)\exp\left\{\frac{i}{2}\left[\int_{t_n}^{t_{n+1}}V(x,t)dt+\tau\beta|U_N^{n+1,2}(x)|^2\right]\right\}, \tag{3.8}$$

where $j=0,1,2,\cdots,N_x$, and $n=0,1,2,\cdots,N_t-1$. $U_N^{n+1,1}(x)$ and $U_N^{n+1,2}(x)=\sum_{j=-2}^{N_x+2}\delta_j^{n+1,2}B_j(x)$ are intermediate results.

3.2. Two-dimensional (2D) scheme

For $d = 2$, Eq (3.2) could be written as

$$i\frac{\partial u}{\partial t}(x,y,t) + \alpha\left(\frac{\partial^2 u}{\partial x^2} + \frac{\partial^2 u}{\partial y^2}\right)(x,y,t) = 0. \tag{3.9}$$

The first-order Lie splitting [10] is applied, and one has

$$i\frac{\partial u}{\partial t}(x,y,t) + \alpha\frac{\partial^2 u}{\partial x^2}(x,y,t) = 0, \tag{3.10}$$

$$i\frac{\partial u}{\partial t}(x,y,t) + \alpha\frac{\partial^2 u}{\partial y^2}(x,y,t) = 0. \tag{3.11}$$

As the operators $\frac{\partial^2}{\partial x^2}$ and $\frac{\partial^2 u}{\partial y^2}$ are commutable, there is no splitting error here.

Similar to Eq (3.5), one can obtain from Eq (3.10) that

$$i\frac{U_N^{n+1}(x,y) - U_N^n(x,y)}{\tau} + \frac{\alpha}{2}\left[U_{Nxx}^{n+1}(x,y) + U_{Nxx}^n(x,y)\right] = 0,$$

where $U_N^n(x,y)$ is the approximation of $u(x,y,t_n)$. Taking $(x,y) = (x_j, y_k)$, it follows from Eqs (2.13) and (2.5) that

$$(i+10\alpha r_x)(\tilde{\delta}_{j-2,k}^{n+1} + \tilde{\delta}_{j+2,k}^{n+1}) + (26i+20\alpha r_x)(\tilde{\delta}_{j-1,k}^{n+1} + \tilde{\delta}_{j+1,k}^{n+1}) + (66i-60\alpha r_x)\tilde{\delta}_{j,k}^{n+1} = iU_N^n(x_j,y_k) - \frac{\tau\alpha}{2}U_{Nxx}^n(x_j,y_k).$$

The above equation is concide benefiting from the new notation $\tilde{\delta}_{j,k}^{n+1}$. Moreover, it forms a (N_x+1) system for each value of k which avoids solving a $(N_x+1)\times(N_y+1)$ system directly. That is the reason why the author applies the splitting method in this paper.

Similarly, it follows from Eq (3.11) that

$$(i+10\alpha r_y)(\hat{\delta}_{j,k-2}^{n+1} + \hat{\delta}_{j,k+2}^{n+1}) + (26i+20\alpha r_y)(\hat{\delta}_{j,k-1}^{n+1} + \hat{\delta}_{j,k+1}^{n+1}) + (66i-60\alpha r_y)\hat{\delta}_{j,k}^{n+1} = iU_N^n(x_j,y_k) - \frac{\tau\alpha}{2}U_{Nyy}^n(x_j,y_k),$$

where $r_y = \tau/h_y^2$.

Consequently, Eqs (3.1)–(3.3) for $d = 2$ could be solved approximately as follows

$$U_N^{n+1,1}(x,y) = U_N^n(x,y)\exp\left\{\frac{i}{2}\left[\int_{t_n}^{t_{n+1}} V(x,y,t)dt + \tau\beta|U_N^n(x,y)|^2\right]\right\}, \tag{3.12}$$

$$(i+10\alpha r_x)(\tilde{\delta}_{j-2,k}^{n+1,2} + \tilde{\delta}_{j+2,k}^{n+1,2}) + (26i+20\alpha r_x)(\tilde{\delta}_{j-1,k}^{n+1,2} + \tilde{\delta}_{j+1,k}^{n+1,2}) + (66i-60\alpha r_x)\tilde{\delta}_{j,k}^{n+1,2}$$
$$= iU_N^{n+1,1}(x_j,y_k) - \frac{\tau\alpha}{2}U_{Nxx}^{n+1,1}(x_j,y_k), \tag{3.13}$$

$$(i+10\alpha r_y)(\hat{\delta}_{j,k-2}^{n+1,3} + \hat{\delta}_{j,k+2}^{n+1,3}) + (26i+20\alpha r_y)(\hat{\delta}_{j,k-1}^{n+1,3} + \hat{\delta}_{j,k+1}^{n+1,3}) + (66i-60\alpha r_y)\hat{\delta}_{j,k}^{n+1,3}$$
$$= iU_N^{n+1,2}(x_j,y_k) - \frac{\tau\alpha}{2}U_{Nyy}^{n+1,2}(x_j,y_k), \tag{3.14}$$

$$U_N^{n+1}(x,y) = U_N^{n+1,3}(x,y)\exp\left\{\frac{i}{2}\left[\int_{t_n}^{t_{n+1}} V(x,y,t)dt + \tau\beta|U_N^{n+1,3}(x,y)|^2\right]\right\}, \tag{3.15}$$

where $j = 0,1,2,\cdots,N_x$, $k = 0,1,2,\cdots,N_y$, and $n = 0,1,2,\cdots,N_t-1$. $U_N^{n+1,1}(x,y)$ and

$$U_N^{n+1,2}(x,y) = \sum_{j=-2}^{N_x+2}\sum_{k=-2}^{N_y+2}\delta_{j,k}^{n+1,2}B_j(x)B_k(y),\ U_N^{n+1,3}(x,y) = \sum_{j=-2}^{N_x+2}\sum_{k=-2}^{N_y+2}\delta_{j,k}^{n+1,3}B_j(x)B_k(y)$$

are intermediate results.

3.3. Three-dimensional (3D) scheme

For $d = 3$, Eq (3.2) could be written as

$$i\frac{\partial u}{\partial t}(x,y,z,t) + \alpha\left(\frac{\partial^2 u}{\partial x^2} + \frac{\partial^2 u}{\partial y^2} + \frac{\partial^2 u}{\partial z^2}\right)(x,y,z,t) = 0. \tag{3.16}$$

It follows from the Lie splitting [10] that

$$i\frac{\partial u}{\partial t}(x,y,z,t) + \alpha\frac{\partial^2 u}{\partial x^2}(x,y,z,t) = 0, \tag{3.17}$$

$$i\frac{\partial u}{\partial t}(x,y,z,t) + \alpha\frac{\partial^2 u}{\partial y^2}(x,y,z,t) = 0, \tag{3.18}$$

$$i\frac{\partial u}{\partial t}(x,y,z,t) + \alpha\frac{\partial^2 u}{\partial z^2}(x,y,z,t) = 0. \tag{3.19}$$

Similar to the 2D case, Eqs (3.1)–(3.3) for $d = 3$ could be solved approximately as follows

$$U_N^{n+1,1}(x,y,z) = U_N^n(x,y,z)\exp\left\{\frac{i}{2}\left[\int_{t_n}^{t_{n+1}} V(x,y,z,t)dt + \tau\beta|U_N^n(x,y,z)|^2\right]\right\}, \tag{3.20}$$

$$\begin{aligned}&(i + 10\alpha r_x)(\tilde{\delta}_{j-2,k,l}^{n+1,2} + \tilde{\delta}_{j+2,k,l}^{n+1,2}) + (26i + 20\alpha r_x)(\tilde{\delta}_{j-1,k,l}^{n+1,2} + \tilde{\delta}_{j+1,k,l}^{n+1,2}) + (66i - 60\alpha r_x)\tilde{\delta}_{j,k,l}^{n+1,2}\\ &= iU_N^{n+1,1}(x_j,y_k,z_l) - \frac{\tau\alpha}{2}U_{Nxx}^{n+1,1}(x_j,y_k,z_l),\end{aligned} \tag{3.21}$$

$$\begin{aligned}&(i + 10\alpha r_y)(\hat{\delta}_{j,k-2,l}^{n+1,3} + \hat{\delta}_{j,k+2,l}^{n+1,3}) + (26i + 20\alpha r_y)(\hat{\delta}_{j,k-1,l}^{n+1,3} + \hat{\delta}_{j,k+1,l}^{n+1,3}) + (66i - 60\alpha r_y)\hat{\delta}_{j,k,l}^{n+1,3}\\ &= iU_N^{n+1,2}(x_j,y_k,z_l) - \frac{\tau\alpha}{2}U_{Nyy}^{n+1,2}(x_j,y_k,z_l),\end{aligned} \tag{3.22}$$

$$\begin{aligned}&(i + 10\alpha r_z)(\check{\delta}_{j,k,l-2}^{n+1,4} + \check{\delta}_{j,k,l+2}^{n+1,4}) + (26i + 20\alpha r_z)(\check{\delta}_{j,k,l-1}^{n+1,4} + \check{\delta}_{j,k,l+1}^{n+1,4}) + (66i - 60\alpha r_z)\check{\delta}_{j,k,l}^{n+1,4}\\ &= iU_N^{n+1,3}(x_j,y_k,z_l) - \frac{\tau\alpha}{2}U_{Nzz}^{n+1,3}(x_j,y_k,z_l),\end{aligned} \tag{3.23}$$

$$U_N^{n+1}(x,y,z) = U_N^{n+1,4}(x,y,z)\exp\left\{\frac{i}{2}\left[\int_{t_n}^{t_{n+1}} V(x,y,z,t)dt + \tau\beta|U_N^{n+1,4}(x,y,z)|^2\right]\right\}, \tag{3.24}$$

where $j = 0,1,2,\cdots,N_x$, $k = 0,1,2,\cdots,N_y$, $l = 0,1,2,\cdots,N_z$, and $n = 0,1,2,\cdots,N_t - 1$. $U_N^{n+1,1}(x,y,z)$ and

$$U_N^{n+1,2}(x,y,z) = \sum_{j=-2}^{N_x+2}\sum_{k=-2}^{N_y+2}\sum_{l=-2}^{N_z+2}\delta_{j,k,l}^{n+1,2}B_j(x)B_k(y)B_l(z), \tag{3.25}$$

$$U_N^{n+1,3}(x,y,z) = \sum_{j=-2}^{N_x+2}\sum_{k=-2}^{N_y+2}\sum_{l=-2}^{N_z+2}\delta_{j,k,l}^{n+1,3}B_j(x)B_k(y)B_l(z), \tag{3.26}$$

$$U_N^{n+1,4}(x,y,z) = \sum_{j=-2}^{N_x+2}\sum_{k=-2}^{N_y+2}\sum_{l=-2}^{N_z+2}\delta_{j,k,l}^{n+1,4}B_j(x)B_k(y)B_l(z) \tag{3.27}$$

are intermediate results.

4. Solvability, conservation and linear stability

In this section, solvability, conservation and linear stability are considered for the numerical methods. The 1D scheme is discussed in details, and the results could be extended to the 2D and 3D ones similarly.

From Eq (3.7), there are $N_x + 1$ equations with $N_x + 5$ unknows. So four additional equations are required. It follows from the periodic boundary condition (1.3) with $d = 1$ that

$$\frac{\partial^m u}{\partial x^m}(x + L_x, t) = \frac{\partial^m u}{\partial x^m}(x, t), m = 0, 1, 2, 3, 4.$$

Taking $x = x_L$, one reaches

$$\begin{aligned}
&\delta_{-2}^{n+1,2}(t) + 26\delta_{-1}^{n+1,2}(t) + 66\delta_{0}^{n+1,2}(t) + 26\delta_{1}^{n+1,2}(t) + \delta_{2}^{n+1,2}(t)\\
=\ &\delta_{N_x-2}^{n+1,2}(t) + 26\delta_{N_x-1}^{n+1,2}(t) + 66\delta_{N_x}^{n+1,2}(t) + 26\delta_{N_x+1}^{n+1,2}(t) + \delta_{N_x+2}^{n+1,2}(t), \qquad (4.1)\\
&-\delta_{-2}^{n+1,2}(t) - 10\delta_{-1}^{n+1,2}(t) + 10\delta_{1}^{n+1,2}(t) + \delta_{2}^{n+1,2}(t)\\
=\ &-\delta_{N_x-2}^{n+1,2}(t) - 10\delta_{N_x-1}^{n+1,2}(t) + 10\delta_{N_x+1}^{n+1,2}(t) + \delta_{N_x+2}^{n+1,2}(t), \qquad (4.2)\\
&\delta_{-2}^{n+1,2}(t) + 2\delta_{-1}^{n+1,2}(t) - 6\delta_{0}^{n+1,2}(t) + 2\delta_{1}^{n+1,2}(t) + \delta_{2}^{n+1,2}(t)\\
=\ &\delta_{N_x-2}^{n+1,2}(t) + 2\delta_{N_x-1}^{n+1,2}(t) - 6\delta_{N_x}^{n+1,2}(t) + 2\delta_{N_x+1}^{n+1,2}(t) + \delta_{N_x+2}^{n+1,2}(t), \qquad (4.3)\\
&-\delta_{-2}^{n+1,2}(t) + 2\delta_{-1}^{n+1,2}(t) - 2\delta_{1}^{n+1,2}(t) + \delta_{2}^{n+1,2}(t)\\
=\ &-\delta_{N_x-2}^{n+1,2}(t) + 2\delta_{N_x-1}^{n+1,2}(t) - 2\delta_{N_x+1}^{n+1,2}(t) + \delta_{N_x+2}^{n+1,2}(t), \qquad (4.4)\\
&\delta_{-2}^{n+1,2}(t) - 4\delta_{-1}^{n+1,2}(t) + 6\delta_{0}^{n+1,2}(t) - 4\delta_{1}^{n+1,2}(t) + \delta_{2}^{n+1,2}(t)\\
=\ &\delta_{N_x-2}^{n+1,2}(t) - 4\delta_{N_x-1}^{n+1,2}(t) + 6\delta_{N_x}^{n+1,2}(t) - 4\delta_{N_x+1}^{n+1,2}(t) + \delta_{N_x+2}^{n+1,2}(t), \qquad (4.5)
\end{aligned}$$

by using Eqs (2.3)–(2.7). It follows from Eqs (4.1)–(4.5) that

$$\delta_{-2}^{n+1,2} = \delta_{N_x-2}^{n+1,2},\ \delta_{-1}^{n+1,2} = \delta_{N_x-1}^{n+1,2},\ \delta_{0}^{n+1,2} = \delta_{N_x}^{n+1,2},\ \delta_{1}^{n+1,2} = \delta_{N_x+1}^{n+1,2},\ \delta_{2}^{n+1,2} = \delta_{N_x+2}^{n+1,2}. \qquad (4.6)$$

Therefore, Eqs (3.7) combined with (4.6) could be rewritten as

$$(iA + 10\alpha r_x B)\delta^{n+1,2} = (iA - 10\alpha r_x B)\delta^{n+1,1}, \qquad (4.7)$$

where

$$A = \begin{pmatrix}
66 & 26 & 1 & 0 & 0 & \cdots & 1 & 26\\
26 & 66 & 26 & 1 & 0 & \cdots & 0 & 1\\
1 & 26 & 66 & 26 & 1 & \cdots & 0 & 0\\
 & \ddots & \ddots & \ddots & \ddots & \ddots & & \\
 & & \ddots & \ddots & \ddots & \ddots & \ddots & \\
0 & 0 & \cdots & 1 & 26 & 66 & 26 & 1\\
1 & 0 & \cdots & 0 & 1 & 26 & 66 & 26\\
26 & 1 & \cdots & 0 & 0 & 1 & 26 & 66
\end{pmatrix}_{N_x \times N_x}, \qquad (4.8)$$

$$B = \begin{pmatrix} -6 & 2 & 1 & 0 & 0 & \cdots & 1 & 2 \\ 2 & -6 & 2 & 1 & 0 & \cdots & 0 & 1 \\ 1 & 2 & -6 & 2 & 1 & \cdots & 0 & 0 \\ & \ddots & \ddots & \ddots & \ddots & \ddots & & \\ & & \ddots & \ddots & \ddots & \ddots & \ddots & \\ 0 & 0 & \cdots & 1 & 2 & -6 & 2 & 1 \\ 1 & 0 & \cdots & 0 & 1 & 2 & -6 & 2 \\ 2 & 1 & \cdots & 0 & 0 & 1 & 2 & -6 \end{pmatrix}_{N_x \times N_x}, \tag{4.9}$$

and

$$\delta^{n+1,m} = \left(\delta_1^{n+1,m}, \delta_2^{n+1,m}, \cdots, \delta_{N_x}^{n+1,m}\right)^\top, m = 1, 2.$$

Lemma 4.1. The circulant matrices A and B respectively have eigenvalues as follows

$$(\lambda_A)_j = 66 + 52\cos\frac{2\pi j}{N_x} + 2\cos\frac{4\pi j}{N_x}, \qquad (\lambda_B)_j = -6 + 4\cos\frac{2\pi j}{N_x} + 2\cos\frac{4\pi j}{N_x},$$

where $j = 0, 1, 2, \cdots, N_x - 1$.

Proof. The eigenvalues could be calculated directly (see [11] and the reference therein). □

Theorem 4.1. The solution of 1D SS5BC schemes (3.6)–(3.8) exists and is unique.

Proof. The coefficient matrix of scheme (3.7) is $M = iA + 10\alpha r_x B$. Using Lemma 4.1, the eigenvalues of M are

$$\begin{aligned} (\lambda_M)_j &= i(\lambda_A)_j + 10\alpha r_x (\lambda_B)_j \\ &= (66i - 60\alpha r_x) + (52i + 40\alpha r_x)\cos\frac{2\pi j}{N_x} + (2i + 20\alpha r_x)\cos\frac{4\pi j}{N_x}, \end{aligned}$$

where $j = 0, 1, 2, \cdots, N_x - 1$. All the eigenvalues are nonzero, so M is invertible and the solution of scheme (3.7) exists and is unique. Moreover, Eqs (3.6) and (3.8) are respectively obtained from Eqs (3.1) and (3.3) exactly. Therefore, the theorem is proved. □

Similarly, one can prove that the solution of 2D SS5BC scheme (3.12)–(3.15) or 3D scheme (3.20)–(3.24) also exists and is unique.

Lemma 4.2. For any $N \times N$ real symmetric matrix C and any complex vector $\delta = (\delta_1, \delta_2, \cdots, \delta_N)^\top$, $\delta^{\mathrm{H}} C\delta$ is real, where δ^{H} is the conjugate transpose of δ and N is a positive integer.

Proof. By matrix operation, one has

$$\delta^{\mathrm{H}} C\delta = \sum_{j=1}^{N}\sum_{k=1}^{N} c_{jk}\bar{\delta}_j\delta_k,$$

where c_{jk} is the element of the matrix lying on the intersection of the jth row and the kth column of C. Since C is a real symmetric matrix, $\delta^{\mathrm{H}} C\delta$ is real. □

Theorem 4.2. The 1D SS5BC schemes (3.6)–(3.8) conserves the discrete quantity

$$Q^n = h_x \sum_{j=1}^{N_x} |U_N^n(x_j)|^2 = h_x \sum_{j=1}^{N_x} |U_N^0(x_j)|^2 = Q^0, \ n = 1, 2, \cdots, N_t. \tag{4.10}$$

Proof. It follows from Eqs (3.6) and (3.8) that $\left|U_N^{n+1,1}(x)\right| = \left|U_N^n(x)\right|$ and $\left|U_N^{n+1}(x)\right| = \left|U_N^{n+1,2}(x)\right|$. So

$$h_x \sum_{j=1}^{N_x} |U_N^{n+1,1}(x_j)|^2 = h_x \sum_{j=1}^{N_x} |U_N^n(x_j)|^2, \quad h_x \sum_{j=1}^{N_x} |U_N^{n+1}(x_j)|^2 = h_x \sum_{j=1}^{N_x} |U_N^{n+1,2}(x_j)|^2, \tag{4.11}$$

where $n = 0, 1, 2, \cdots, N_t - 1$.

Equation (4.7) is rewritten as

$$iA\left(\delta^{n+1,2} - \delta^{n+1,1}\right) + 10\alpha r_x B\left(\delta^{n+1,2} + \delta^{n+1,1}\right) = 0. \tag{4.12}$$

Multiplying Eq (4.12) by $\left[A\left(\delta^{n+1,2} + \delta^{n+1,1}\right)\right]^{\mathrm{H}}$ and taking the imaginary part, one has

$$Re\left[\left(\delta^{n+1,2} + \delta^{n+1,1}\right)^{\mathrm{H}} A^2\left(\delta^{n+1,2} - \delta^{n+1,1}\right)\right] + 10\alpha r_x Im\left[\left(\delta^{n+1,2} + \delta^{n+1,1}\right)^{\mathrm{H}} AB\left(\delta^{n+1,2} + \delta^{n+1,1}\right)\right] = 0, \tag{4.13}$$

where A^{H} is the conjugate transpose of A, and $A^{\mathrm{H}} = A$ since A is real symmetric. It is obvious that

$$\begin{aligned} & \left(\delta^{n+1,2} + \delta^{n+1,1}\right)^{\mathrm{H}} A^2\left(\delta^{n+1,2} - \delta^{n+1,1}\right) \\ = & \left(\delta^{n+1,2}\right)^{\mathrm{H}} A^2\delta^{n+1,2} - \left(\delta^{n+1,2}\right)^{\mathrm{H}} A^2\delta^{n+1,1} + \left(\delta^{n+1,1}\right)^{\mathrm{H}} A^2\delta^{n+1,2} - \left(\delta^{n+1,1}\right)^{\mathrm{H}} A^2\delta^{n+1,1}. \end{aligned} \tag{4.14}$$

As A^2 is real symmetric and $\left(\delta^{n+1,2}\right)^{\mathrm{H}} A^2\delta^{n+1,1}$ and $\left(\delta^{n+1,1}\right)^{\mathrm{H}} A^2\delta^{n+1,2}$ are conjugate to each other, one gets

$$Re\left[-\left(\delta^{n+1,2}\right)^{\mathrm{H}} A^2\delta^{n+1,1} + \left(\delta^{n+1,1}\right)^{\mathrm{H}} A^2\delta^{n+1,2}\right] = 0.$$

By applying Lemma 4.2, one obtains from Eq (4.14) that

$$Re\left[\left(\delta^{n+1,2} + \delta^{n+1,1}\right)^{\mathrm{H}} A^2\left(\delta^{n+1,2} - \delta^{n+1,1}\right)\right] = \left(\delta^{n+1,2}\right)^{\mathrm{H}} A^2\delta^{n+1,2} - \left(\delta^{n+1,1}\right)^{\mathrm{H}} A^2\delta^{n+1,1}. \tag{4.15}$$

Moreover, as AB is a real symmetric matrix, one can obtain from Lemma 4.2 that

$$Im\left[\left(\delta^{n+1,2} + \delta^{n+1,1}\right)^{\mathrm{H}} AB\left(\delta^{n+1,2} + \delta^{n+1,1}\right)\right] = 0. \tag{4.16}$$

It follows from Eqs (4.13), (4.15) and (4.16) that

$$\left(\delta^{n+1,2}A\right)^{\mathrm{H}} A\delta^{n+1,2} = \left(\delta^{n+1,1}A\right)^{\mathrm{H}} A\delta^{n+1,1},$$

i.e.,

$$h_x \sum_{j=1}^{N_x} |U_N^{n+1,2}(x_j)|^2 = h_x \sum_{j=1}^{N_x} |U_N^{n+1,1}(x_j)|^2, \tag{4.17}$$

where

$$A\delta^{n+1,m} = \left(u_N^{n+1,m}(x_1), u_N^{n+1,m}(x_2), \cdots, u_N^{n+1,m}(x_{N_x})\right)^{\top}, m = 1, 2$$

is used. Therefore, it follows from Eqs (4.11) and (4.17) that

$$h_x \sum_{j=1}^{N_x} |U_N^{n+1}(x_j)|^2 = h_x \sum_{j=1}^{N_x} |U_N^n(x_j)|^2, n = 0, 1, 2, \cdots, N_t - 1.$$

Thus, Eq (4.10) is reached. □

Similarly, the 2D SS5BC schemes (3.12)–(3.15) and the 3D schemes (3.20)–(3.24) also respectively preserve the discrete quantity as follows

$$Q^n = h_x h_y \sum_{j=1}^{N_x}\sum_{k=1}^{N_y} |U_N^n(x_j, y_k)|^2 = h_x h_y \sum_{j=1}^{N_x}\sum_{k=1}^{N_y} |U_N^0(x_j, y_k)|^2 = Q^0, \tag{4.18}$$

$$Q^n = h_x h_y h_z \sum_{j=1}^{N_x}\sum_{k=1}^{N_y}\sum_{l=1}^{N_z} |U_N^n(x_j, y_k, z_l)|^2 = h_x h_y h_z \sum_{j=1}^{N_x}\sum_{k=1}^{N_y}\sum_{l=1}^{N_z} |U_N^0(x_j, y_k, z_l)|^2 = Q^0, \tag{4.19}$$

$n = 1, 2, \cdots, N_t$.

Next, the linear stability of the SS5BC scheme is considered.

Theorem 4.3. The 1D SS5BC schemes (3.6)–(3.8) is unconditionally stable.

Proof. Substituting $U_N^n = \xi^n e^{i\beta_1 x}$ and $U_N^{n+1,1} = \xi^{n+1,1} e^{i\beta_1 x}$ into Eq (3.6), one gets $\xi^{n+1,1} = G_1 \xi^n$, where

$$G_1 = \exp\left\{\frac{i}{2}\left[\int_{t_n}^{t_{n+1}} V(x,t)dt + \tau\beta|\xi^n|^2\right]\right\}.$$

Similarly, it follows from Eq (3.8) that $\xi^{n+1} = G_3 \xi^{n+1,2}$, where

$$G_3 = \exp\left\{\frac{i}{2}\left[\int_{t_n}^{t_{n+1}} V(x,t)dt + \tau\beta|\xi^{n+1,2}|^2\right]\right\}.$$

Equation (3.7) chould be rewritten as

$$iU_N^{n+1,2}(x_j) + \frac{\tau\alpha}{2} U_{Nxx}^{n+1,2}(x_j) = iU_N^{n+1,1}(x_j) - \frac{\tau\alpha}{2} U_{Nxx}^{n+1,1}(x_j).$$

Plugging $U_N^{n+1,2} = \xi^{n+1,2} e^{i\beta_1 x}$ into the above equation, one has $\xi^{n+1,2} = G_2 \xi^{n+1,1}$, where

$$G_2 = \frac{2i - \tau\alpha\beta_1^2}{2i + \tau\alpha\beta_1^2}.$$

So $\xi^{n+1} = G\xi^n$, where $G = G_3 G_2 G_1$. Thus, the 1D SS5BC scheme is unconditionally stable, since $|G| = 1$. □

Similarly, one can obtain that the 2D and 3D SS5BC schemes are also unconditionally stable.

5. Numerical experiments

Denote

$$\|e\|_\infty = \max_{j,k,l,n} |U_N^n(x_j, y_k, z_l) - u(x_j, y_k, z_l, t_n)|$$

be the maximum error. For convenience, we take $N = N_x = N_y = N_z$ and $h = h_x = h_y = h_z$. The convergence order is approximated as

$$Order\ of\ convergence \approx \frac{log\left(\|e\|_\infty(h_1)/\|e\|_\infty(h_2)\right)}{log\left(h_1/h_2\right)},$$

where $\|e\|_\infty(h_1)$ is the maximum error corresponding to the step size h_1.

5.1. Test 1

Take $\alpha = \frac{1}{2}$ and $\beta = -1$. For $d = 1$, Eq (1.1) has an exact solution

$$u(x,t) = \sin(2\pi x)e^{-it},$$

with

$$V(x) = -1 + 2\pi^2 + \sin^2(2\pi x).$$

For $d = 2$, Eq (1.1) has an exact solution

$$u(x,y,t) = \sin(2\pi x)\sin\left(2\pi y + \frac{\pi}{4}\right)e^{-it},$$

with

$$V(x,y) = -1 + 4\pi^2 + \sin^2(2\pi x)\sin^2\left(2\pi y + \frac{\pi}{4}\right).$$

And Eq (1.1) with $d = 3$ has an exact solution

$$u(x,y,z,t) = \sin(2\pi x)\sin\left(2\pi y + \frac{\pi}{2}\right)\sin\left(2\pi z + \frac{\pi}{4}\right)e^{-it},$$

with

$$V(x,y,z) = -1 + 6\pi^2/2 + \sin^2(2\pi x)\sin^2(2\pi y + \frac{\pi}{2})\sin^2(2\pi z + \frac{\pi}{4}).$$

The initial condition (1.2) could be given according to the exact solution. Take $\mathbf{x} \in [0,1]^d$ and $T = 1$. As $V(\mathbf{x},t) = V(\mathbf{x})$ independent of t, we have

$$\int_{t_n}^{t_{n+1}} V(\mathbf{x},t)dt = \tau V(\mathbf{x})$$

in the nonlinear schemes. And the linear schemes are solved by the Douple-Sweep method.

It follows from the results in [12] that

$$\|S_3^{(r)} - f^{(r)}\|_\infty \le \epsilon_r \|f^{(4)}\|_\infty h^{4-r}, r = 0,1,2,3,$$
$$\|S_5^{(r)} - f^{(r)}\|_\infty \le \tilde{\epsilon}_r \|f^{(6)}\|_\infty h^{6-r}, r = 0,1,2,\cdots,5,$$

where S_3 and S_5 are respectively the cubic spline and quintic spline associated with the function f. So the accuracy order of the SS3BC scheme in [7] and the SS5BC scheme in this paper might be $O(\tau^2+h^2)$ and $O(\tau^2 + h^4)$, respectively.

The above three examples are applied to verify the convergence order of the proposed SS5BC scheme and the SS3BC scheme in [7]. Thus we take $\tau = h^2$ for the SS5BC scheme, and $\tau = h$ for the SS3BC one. The numerical results are listed in Tables 1 and 2, respectively. Table 1 shows that all the 1D, 2D and 3D SS5BC schemes are convergent with second-order in time and fourth-order in space, and Table 2 shows that all the 1D, 2D and 3D SS3BC schemes are convergent with second-order both in time and in space. So the proposed SS5BC schemes do improve the accuracy order compared with the SS3BC schemes [7], which is the aim of this paper.

Table 1. Error and convergence rate of the SS5BC scheme.

	1D		2D		3D	
h	$\|\|e\|\|_\infty$	rate	$\|\|e\|\|_\infty$	rate	$\|\|e\|\|_\infty$	rate
1/10	5.62e-2	-	1.11e-1	-	1.66e-1	-
1/20	3.73e-3	3.91	7.37e-3	3.91	1.11e-2	3.91
1/40	2.34e-4	3.99	4.67e-4	3.98	7.01e-4	3.98
1/80	1.46e-5	4.00	2.92e-5	4.00	4.38e-5	4.00

Table 2. Error and convergence rate of the SS3BC scheme.

	1D		2D		3D	
h	$\|\|e\|\|_\infty$	rate	$\|\|e\|\|_\infty$	rate	$\|\|e\|\|_\infty$	rate
1/20	1.19	-	1.88	-	1.96	-
1/40	3.46e-1	1.78	6.82e-1	1.47	9.98e-1	0.97
1/80	8.92e-2	1.96	1.78e-1	1.94	2.67e-1	1.90
1/160	2.25e-2	1.99	4.49e-2	1.99	6.73e-2	1.99

In the above tests, the SS5BC scheme possesses higher order of accuracy than the SS3BC one. However, the coefficient matrix is five diagonal for the former scheme while tridiagonal for the later one, and it seems that the SS5BC scheme might cost more. For further comparison, the computing time is compared between the two kinds of methods. For the above three examples, one attaines $||e||_\infty < 0.002$ when the step sizes are free [13]. Take $\mathbf{x} \in [0, 1]^d$ and $T = 0.5$. Table 3 shows that the SS5BC methods are more efficient than the SS3BC ones since the formers cost less time.

Table 3. Comparison of computing time to attain $||e||_\infty < 0.002$.

	SS5BC			SS3BC		
N	h, τ	$\|\|e\|\|_\infty$	CPU(s)	h, τ	$\|\|e\|\|_\infty$	CPU(s)
1D	1/20,0.0025	1.95e-3	0.06	1/64,0.00556	1.96e-3	0.20
2D	1/20,0.0018	1.96e-3	1.97	1/64,0.00527	1.94e-3	4.83
3D	1/20,0.00158	1.96e-3	72.70	1/64,0.00517	1.92e-3	236.95

The conserved quantity $Q(t)$ is respectively simulated for $d = 1, 2, 3$, seeing Eqs (4.10), (4.18) and (4.19). Taking $\mathbf{x} \in [0, 1]^d, h = 0.05, \tau = 0.02$ and $T = 5$, the values of Q^n at $t = 0, 1, 2, 3, 4, 5$ are listed in Table 4. It follows from the table that the 1D, 2D and 3D SS5BC schemes remain the conserved quantity Q^n very well.

Table 4. Conserved quintity Q^n with various values of t.

t	1D	2D	3D
0	0.500000000000000	0.262500000000001	0.144375000000000
1	0.499999999999994	0.262499999999998	0.144375000000000
2	0.499999999999990	0.262499999999998	0.144375000000001
3	0.499999999999987	0.262499999999998	0.144375000000002
4	0.499999999999984	0.262499999999998	0.144375000000003
5	0.499999999999983	0.262499999999998	0.144375000000003

5.2. Test 2

Take $\alpha = \frac{1}{2}$ and $\beta = -1$. For $d = 1$, Eq (1.1) has a soliton solution

$$u(x,t) = exp[-(x-t)^2 + i(x-t)],$$

with

$$V(x,t) = \frac{1}{2} - 2(x-t)^2 + exp[-2(x-t)^2].$$

For $d = 2$, Eq (1.1) has a soliton solution

$$u(x,y,t) = exp[-(x-t)^2 - (y-t)^2 + i(x+y-t)],$$

with

$$V(x,y,t) = 2 - 2(x-t)^2 - 2(y-t)^2 + exp[-2(x-t)^2 - 2(y-t)^2].$$

For $d = 3$, Eq (1.1) has a soliton solution

$$u(x,y,z,t) = exp[-(x-t)^2 - (y-t)^2 - (z-t)^2 + i(x+y+z-t)],$$

with

$$V(x,y,t) = \frac{7}{2} - 2(x-t)^2 - 2(y-t)^2 - 2(z-t)^2 + exp[-2(x-t)^2 - 2(y-t)^2 - 2(z-t)^2].$$

The initial condition $u(\mathbf{x}, 0)$ in Eq (1.2) could be given according to the exact solutions. Since $V(\mathbf{x}, t)$ can not be integrated exactly, one may apply the following approximation

$$\int_{t_n}^{t_{n+1}} V(\mathbf{x}, t)dt \approx \tau V(\mathbf{x}, t_n + \frac{\tau}{2})$$

in the schemes. Take $\mathbf{x} \in [-5, 5]^d, t \in [0, 1]$, and $\tau = h^2$. The error and convergence order are listed in Table 5. It shows that the 1D, 2D and 3D SS5BC schemes are convergent with order $O(\tau^2 + h^4)$.

Table 5. Error and convergence rate with $\tau = h^2$.

	1D		2D		3D	
N	$\|\|e\|\|_\infty$	rate	$\|\|e\|\|_\infty$	rate	$\|\|e\|\|_\infty$	rate
50	9.62e-4	-	1.35e-3	-	1.89e-3	-
100	6.01e-5	4.00	8.50e-5	3.99	1.19e-4	3.99
160	9.20e-6	3.99	1.30e-5	4.00	1.81e-5	4.00
200	3.77e-6	4.00	5.32e-6	4.00	7.44e-6	3.99

Taking $\mathbf{x} \in [-5, 10]^d, h = 0.1, \tau = 0.02$ and $T = 5$, the values of Q^n at $t = 0, 1, 2, 3, 4, 5$ are listed in Table 6. The table shows that the 1D, 2D and 3D SS5BC schemes also keep the conserved quantity Q^n well in this test.

Table 6. Conserved quintity Q^n with various values of t.

t	1D	2D	3D
0	1.253314137315500	1.570796326794896	1.968701243215303
1	1.253314137315498	1.570796326794888	1.968701243215286
2	1.253314137315495	1.570796326794880	1.968701243215271
3	1.253314137315492	1.570796326794872	1.968701243215254
4	1.253314137315489	1.570796326794864	1.968701243215238
5	1.253314137315486	1.570796326794855	1.968701243215222

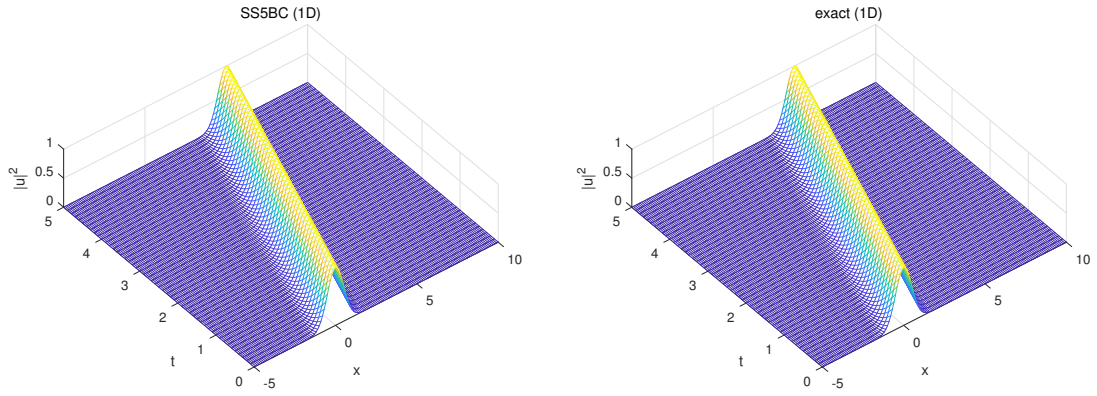

Figure 1. Soliton $|u|^2$ of the 1D NLS equation from $t = 0$ to $t = 5$. Left: numerical. Right: exact.

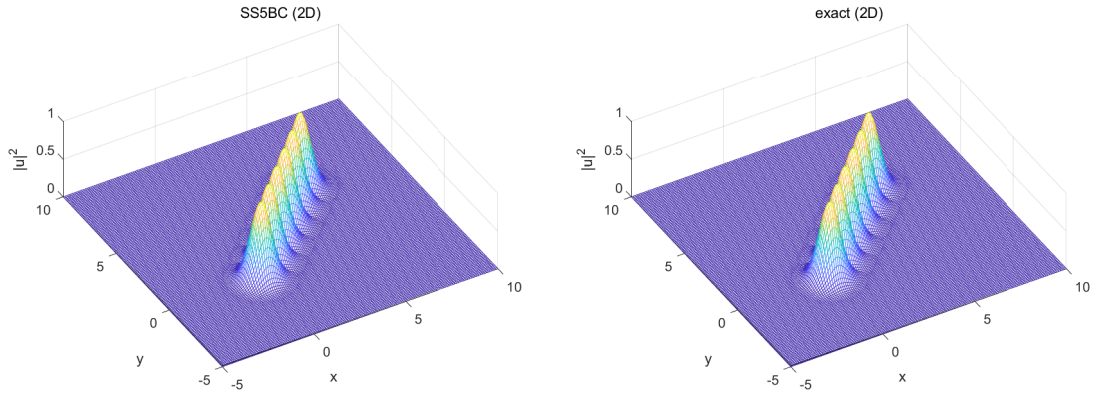

Figure 2. Soliton $|u|^2$ of the 2D NLS equation from $t = 0$ to $t = 5$. Left: numerical. Right: exact.

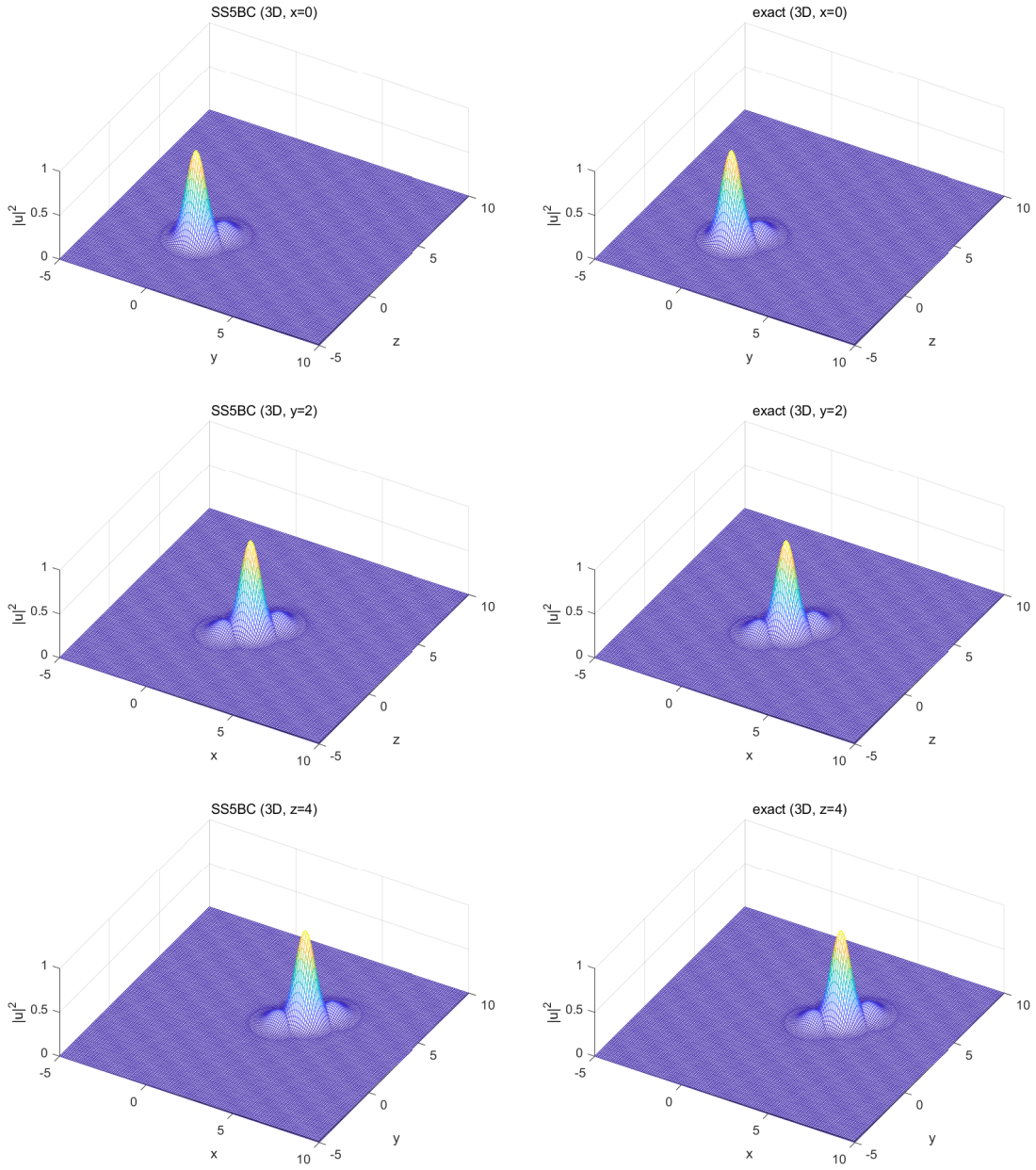

Figure 3. Profiles of $|u|^2$ of the 3D NLS equation from $t = 0$ to $t = 5$ at $x = 0$ (Top), $y = 2$ (Middle) and $z = 4$ (Bottom). Left: numerical. Right: exact.

Numerical simulations of $|u|^2$ computed by the SS5BC schemes are plotted in Figures 1–3. In Figure 1, the 1D solitary wave transfers from the left to the right as time inceases which is in accordance with the exact one. In Figure 2, the 2D solitary waves at $t = 0, 1, 2, 3, 4, 5$ are plotted which also agree with the exact ones. For 3D, profiles of $|u|^2$ at $x = 0, y = 2$ and $z = 4$ are respectively plotted in Figure 3, which are still consistent with the exact ones.

6. Numerical applications

Taking $\alpha = \frac{1}{2}$ and the trap potential

$$V(\mathbf{x}, t) = V(\mathbf{x}) = \begin{cases} -\frac{1}{2}x^2, & d = 1, \\ -\frac{1}{2}\left(x^2 + \gamma_y^2 y^2\right), & d = 2, \\ -\frac{1}{2}\left(x^2 + \gamma_y^2 y^2 + \gamma_z^2 z^2\right), & d = 3, \end{cases} \tag{6.1}$$

the NLS equation (1.1) is known as the Gross-Pitaevskii (GP) equation, which is usually used to model the properties of a Bose-Einstein condensate (BEC) at extremely low temperatures [1, 14]. For normalization [14], the conserved quantity in Eq (1.4) is required as $Q(t) = 1$ for each $t \in [0, T]$.

For $d = 1$, the initial condition (1.2) is chosen as

$$u(x, 0) = \frac{1}{\pi^{1/4}} \exp\left(-\frac{1}{2}x^2\right).$$

The condensate width [14] of 1D BEC is numerically approximated as

$$\sigma^n = \sqrt{h \sum_{j=1}^{N} (x_j - \hat{x})^2 |U_N^n(x_j)|^2},$$

where

$$\hat{x} = h \sum_{j=1}^{N} x_j |U_N^n(x_j)|^2.$$

Take $x \in [-8, 8], T = 10, h = 0.2, \tau = 0.02$, and $\beta = -3$ in Eq (1.1). The approximated condensate density $|u|^2$ and the condensate width σ^n are plotted in Figure 4. And the conserved quantity Q^n listed in Table 7 is about 1, which simulates $Q(t) = 1$ very well.

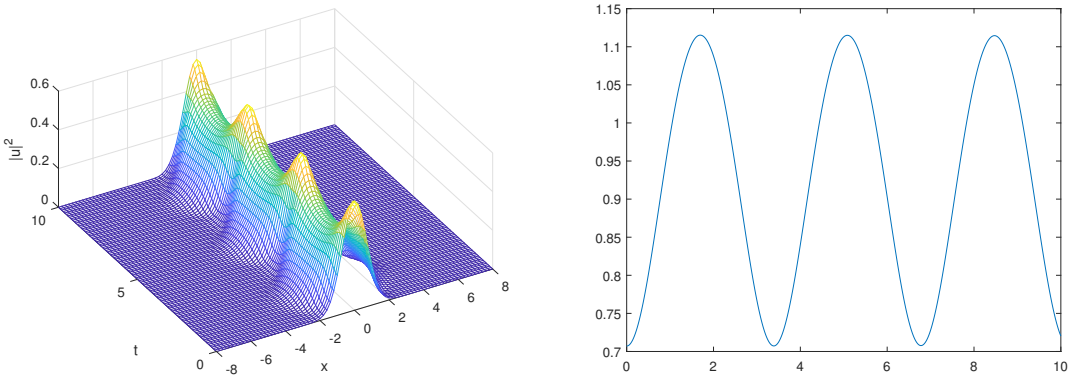

Figure 4. Numerical results of 1D BEC from $t = 0$ to $t = 10$. Left: The evolution of position density. Right: The condensate width as a function of time.

Table 7. Conserved quintity Q^n of 1D BEC with various values of t.

t	Q^n
0	1.000000000000001
2	1.000000000000032
4	1.000000000000063
6	1.000000000000091
8	1.000000000000124
10	1.000000000000155

For $d = 2$, the condensate widths [14] along the x- and y-axes are respectively approximated as

$$\sigma_x^n = \sqrt{h^2 \sum_{j=1}^{N} (x_j - \hat{x})^2 \sum_{k=1}^{N} |U_N^n(x_j, y_k)|^2}, \ \sigma_y^n = \sqrt{h^2 \sum_{k=1}^{N} (y_k - \hat{y})^2 \sum_{j=1}^{N} |U_N^n(x_j, y_k)|^2},$$

where

$$\hat{x} = h^2 \sum_{j=1}^{N} x_j \sum_{k=1}^{N} |U_N^n(x_j, y_k)|^2, \ \hat{y} = h^2 \sum_{k=1}^{N} y_k \sum_{j=1}^{N} |U_N^n(x_j, y_k)|^2.$$

Taking $(x, y) \in [-8, 8]^2, T = 10, h = 0.2, \tau = 0.02$ and $\beta = -2$, two cases are considered as follows:

Case I. Let $\gamma_y = 1$. The initial condition (1.2) is chosen as

$$u(x, y, 0) = \frac{1}{\sqrt{\pi}} \exp\left[-\frac{1}{2}(x^2 + \gamma_y y^2)\right].$$

Case II. Let $\gamma_y = 2$. The initial condition is taken as

$$u(x, y, 0) = \frac{\gamma_y^{1/4}}{\sqrt{2\pi}} \exp\left[-\frac{1}{2}(x^2 + \gamma_y y^2)\right].$$

The approximated condensate widths of Cases I and II are plotted in Figure 5. γ_y is a ratio of the trap frequencies in x- and y-direction [14]. As $\gamma_y = 1$ in Case I, the trap potential (6.1) and also the condensate are isotropic. So the condensate widths along the x- and y-axes should be the same for Case I, which is shown in Figure 5 numerically. The conserved quantities $Q^n \approx 1$ of the two cases are both given in Table 8.

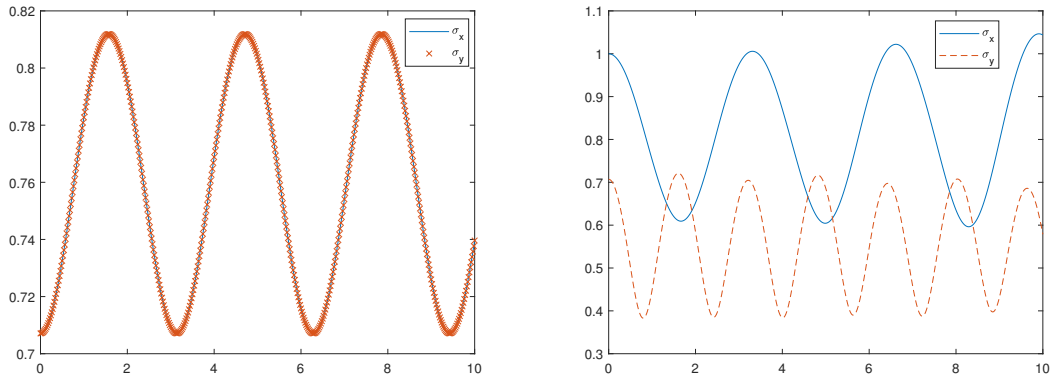

Figure 5. Condensate widths of 2D BECs from $t = 0$ to $t = 10$. Left: Case I. Right: Case II.

Table 8. Conserved quintity Q^n of 2D BECs with various values of t.

t	Case I	Case II
0	1.000000000000001	0.999999999999999
2	1.000000000000061	1.000000000000058
4	1.000000000000121	1.000000000000119
6	1.000000000000179	1.000000000000179
8	1.000000000000238	1.000000000000237
10	1.000000000000296	1.000000000000296

For $d = 3$, the condensate widths [14] along the x-axis is numerically approximated as

$$\sigma_x^n = \sqrt{h^3 \sum_{j=1}^{N} (x_j - \hat{x})^2 \sum_{k=1}^{N} \sum_{l=1}^{N} |U_N^n(x_j, y_k, z_l)|^2},$$

where

$$\hat{x} = h^3 \sum_{j=1}^{N} x_j \sum_{k=1}^{N} \sum_{l=1}^{N} |U_N^n(x_j, y_k, z_l)|^2.$$

Similarly, the condensate widths along the y- and z-axes could be approximated respectively. Take $(x, y, z) \in [-8, 8]^3$, $T = 5$, $h = 0.2$ and $\tau = 0.02$. The initial condition (1.2) is chosen as

$$u(x, y, z, 0) = \frac{(\gamma_y \gamma_z)^{1/4}}{(\pi/4)^{3/4}} \exp\left[-2(x^2 + \gamma_y y^2 + \gamma_z z^2)\right],$$

and the following two cases are considered:

Case I. Let $\beta = -0.1, \gamma_y = 2, \gamma_z = 4$.

Case II. Let $\beta = -1, \gamma_y = 1, \gamma_z = 2$.

In Figure 6, the approximated condensate widths of Cases I and II are plotted. As $\gamma_y = 1$ in Case II, the condensate is symmetric in x- and y-directions, which is shown in Figure 6 that σ_x^n equals σ_y^n. In Table 9, the conserved quantities $Q^n \approx 1$ are listed.

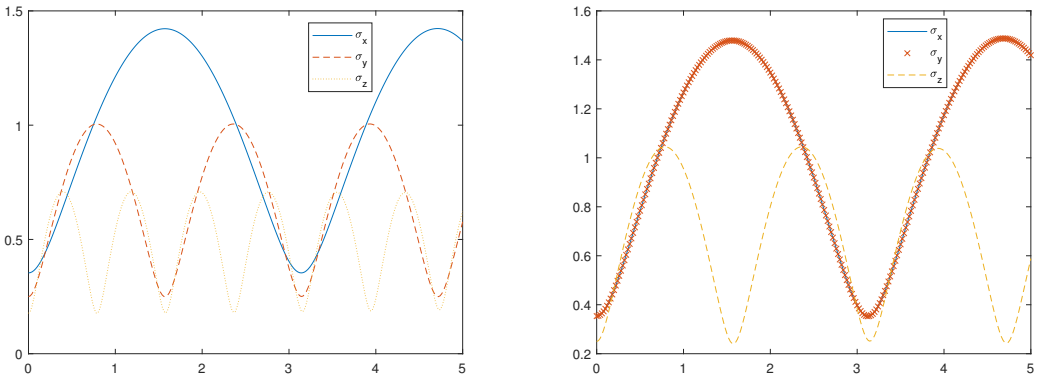

Figure 6. Condensate widths of 3D BECs from $t = 0$ to $t = 5$. Left: Case I. Right: Case II.

Table 9. Conserved quintity Q^n of 3D BECs with various values of t.

t	Case I	Case II
0	1.00000040147946	1.00000000000005
1	1.00000040147932	0.99999999999997
2	1.00000040147934	0.99999999999981
3	1.00000040147932	0.99999999999974
4	1.00000040147947	1.00000000000011
5	1.00000040147944	1.00000000000016

7. Conclusions

In this paper, the SS5BC schemes are proposed for the one-dimensional and multi-dimensional NLS equations. The new notations are introduced for the 2D and 3D equations in order to make the schemes more brief and accomplishable. The solvability, conservation and linear stability are discussed for the methods. Variable numerical experiments and applications are carried out to prove that the present schemes are reliable and efficient. The convergence order, conserved quantity and solitary wave are verified numerically. Finally, the SS5BC methods are applied to study BECs. It is worth to say that the skills of analysis in this paper could also be applied to the SS3BC schemes, and advanced theoretical analyses are still open which are expected in the future work.

Use of AI tools declaration

The authors declare they have not used Artificial Intelligence (AI) tools in the creation of this article.

Acknowledgments

This work is supported by the National Natural Science Foundation of China under Grant No. 11701280.

Conflict of interest

The author declares no conflict of interest in this paper.

References

1. H. Wang, Numerical studies on the split-step finite difference method for nonlinear Schrödinger equations, *Appl. Math. Comput.*, **170** (2005), 17–35. http://doi.org/10.1016/j.amc.2004.10.066
2. H. Wang, X. Ma, J. Lu, W. Gao, An efficient time-splitting compact finite difference method for Gross-Pitaevskii equation, *Appl. Math. Comput.*, **297** (2017), 131–144. http://dx.doi.org//10.1016/j.amc.2016.10.037
3. L. Li, A split-step finite-element method for incompressible Navier-Stokes equations with high-order accuracy up-to the boundary, *J. Comput. Phys.*, **408** (2020), 109274. http://doi.org/10.1016/j.jcp.2020.109274
4. Y. Gao, L. Mei, Time-splitting Galerkin method for spin-orbit-coupled Bose-Einstein condensates, *Comput. Math. Appl.*, **87** (2021), 77–90. http://doi.org/10.1016/j.camwa.2021.02.009
5. W. Bao, H. Li, J. Shen, A generalized-Laguerre-Fourier-Hermite pseudospectral method for computing the dynamics of rotating Bose-Einstein condensates, *SIAM J. Sci. Comput.*, **31** (2009), 3685–3711. http://doi.org/10.1137/080739811
6. W. Bao, Y. Cai, Y. Feng, Improved uniform error bounds on time-splitting methods for long-time dynamics of the nonlinear Klein-Gordon equation with weak nonlinearity, *SIAM J. Numer. Anal.*, **60** (2022), 1962–1984. http://doi.org/10.1137/21M1449774
7. S. Wang, L. Zhang, Split-step cubic B-spline collocation methods for nonlinear Schrödinger equations in one, two, and three dimensions with Neumann boundary conditions, *Numer. Algorithms*, **81** (2019), 1531–1546. http://doi.org/10.1007/s11075-019-00762-2
8. D. Irk, *İ*. Dağ, Quintic B-spline collocation method for the generalized nonlinear Schrödinger equation, *J. Frankl. Inst.*, **348** (2011), 378–392. http://doi.org/10.1016/j.jfranklin.2010.12.004
9. G. Strang, On the construction and comparison of difference schemes, *SIAM J. Numer. Anal.*, **5** (1968), 506–517. https://doi.org/10.1137/0705041
10. S. Yu, S. Zhao, G. W. Wei, Local spectral time splitting method for first- and second-order partial differential equations, *J. Comput. Phys.*, **206** (2005), 727–780. http://doi.org/10.1016/j.jcp.2005.01.010
11. T. Wang, B. Guo, Q. Xu, Fourth-order compact and energy conservative difference schemes for the nonlinear Schrödinger equation in two dimensions, *J. Comput. Phys.*, **243** (2013), 382–399. http://dx.doi.org/10.1016/j.jcp.2013.03.007
12. C. A. Hall, On error bounds for spline interpolation, *J. Approx. Theory*, **1** (1968), 209–218. https://doi.org/10.1016/0021-9045(68)90025-7

13. T. R. Taha, M. I. Ablowitz, Analytical and numerical aspects of certain nonlinear evolution equations. II: Numerical, nonlinear Schrödinger equations, *J. Comput. Phys.*, **55** (1984), 203–230. http://doi.org/10.1016/0021-9991(84)90003-2

14. W. Bao, D. Jaksch, P. A. Markowich, Numerical solution of the Gross-Pitaevskii equation for Bose-Einstein condensation, *J. Comput. Phys.*, **187** (2003), 318–342. http://doi.org/10.1016/S0021-9991(03)00102-5

AIMS Press